submitted to *Geophys. J. Int.*

Crustal structure of the Iceland region from spectrally correlated free-air and terrain gravity data

T.E. Leftwich[1], R.R.R.B. von Frese[1], L.V. Potts[2], D.R. Roman[3] and P.T. Taylor[4]

[1] *Dept. of Geological Sciences, The Ohio State University, Columbus, OH 43210*

[2] *Dept. of Civil and Environmental Engineering and Geodetic Science, The Ohio State University, Columbus, OH*

[3] *National Oceanic and Atmospheric Administration, National Geodetic Survey, Silver Springs, MD 20910-3282*

[4] *NASA Geodynamics Branch (Code 921), Goddard Space Flight Center, Greenbelt MD 20771*

Received 2002 Dec 00; 00000

SUMMARY

Seismic refraction studies have provided critical, but spatially restricted constraints on the structure of the Icelandic crust. To obtain a more comprehensive regional view of this tectonically complicated area, we spectrally correlated free-air gravity anomalies against computed gravity effects of the terrain for a crustal thickness model that also conforms to regional seismic and thermal constraints. Our regional crustal thickness estimates suggest thickened crust extends up to 500 km on either side of the Greenland-Scotland Ridge with the Iceland-Faeroe Ridge crust being less extended and on average 3-5 km thinner than the crust of the Greenland-Iceland Ridge. Crustal thickness estimates for Iceland range from 25-35 km in conformity with seismic predictions of a cooler, thicker crust. However, the deepening of our gravity-inferred Moho relative to seismic estimates at the thermal plume and rift zones of Iceland suggests partial melting. The amount of partial melting may range from about 8% beneath the rift zones to perhaps 20% above the plume core where mantle temperatures may be 200-400°C above normal. Beneath Iceland, areally limited regions of partial melting may also be compositionally and mechanically layered

and intruded. The mantle plume appears to be centered at (64.6°N, 17.4°W) near the Vatnajökull Glacier and the central Icelandic neovolcanic zones.

Key words: Iceland, Greenland-Scotland Ridge, gravity anomalies, crustal thickness, heat flow, partial melting, tectonics.

1 INTRODUCTION

Iceland and its extended ridges involve thickened oceanic crust that straddles the spreading Mid-Atlantic Ridge and a mantle plume off the ridge axis to the southeast (Fig. 1). The Reykjanes Ridge is part of the Mid-Atlantic Ridge system that extends southwest of Iceland, while the Kolbeinsey Ridge is the continuation of the Mid-Atlantic Ridge northeast of Iceland. The Greenland-Iceland Ridge and the Iceland-Faeroe Ridge are parts of the shallow transverse rise that runs northwestwards towards Greenland and southeastwards towards the Faeroe Islands across the northeastern Atlantic. Iceland and these aseismic trans-Atlantic ridges extending from Iceland were created by seafloor spreading that originated about 55 Ma above abnormally hot mantle (Bott & Gunnarsson 1980; White 1992). Higher than normal temperatures produced greater melt volumes that enhanced crustal thickening (e.g., White et al. 1992; Smallwood et al. 1995). Within Iceland, southwest-northeast trending neovolcanic Eastern and Western Rift Zones (**ERZ** and **WRZ** in Fig. 1) reflect unique sub-aerial expressions of mid-oceanic rifting from which the North American and Eurasian Plates diverge (e.g., Jancin 1985; Oskarsson et al. 1985).

Geophysical investigations provide critical information on the nature of the crust in this oceanic region where only the surface geology on Iceland is exposed. For Iceland, previous seismic, magnetotelluric, and resistivity studies predicted thin crust with partial melt regions at depths of 10-15 km beneath the neovolcanic zones (e.g., Beblo & Björnsson, 1980; Eysteinsson & Hermance 1985; Schmeling 1985). However, subsequent reinterpretations of these data based on more recent seismic studies suggested the crust was cooler and perhaps up to 20 km thicker (e.g., Menke & Levin 1994; Staples et al. 1997; Smallwood et al. 1999). These ambiguities in the Moho estimations within the rifted regions and in the vicinity of the

Iceland Plume may partly reflect difficulties in accounting for the seismic velocity effects of temperature, as well as fracturing, faulting, and other complicating features in the relatively young igneous rocks.

Crustal thicknesses in excess of 20-25 km were seismically inferred for central and southwestern Iceland (Bjarnson et al. 1993; Menke & Levin 1994), although thinner estimates within the Reykjanes rift zone were also found (Weir et al. 1998, 2001). A seismic Moho depth of 24 km was obtained for northeastern Iceland (Staples et al. 1997). Seismic Moho estimates for eastern and western Iceland range up to 35 km (Menke 1999). Additional seismic and rare earth element inversions are also congruent with Icelandic crustal thickness estimates of 20-25 km (McKenzie 1984; Sleep 1990; White et al. 1992). Seismic (Darbyshire et al. 1998) and gravity (Darbyshire et al. 2000a; b) analyses inferred a thickening of the Icelandic crust to about 40 km above the plume's center.

Seismic studies of the Iceland-Faeroe Ridge indicated crustal thicknesses of perhaps 25-30 km (Bott & Gunnarsson, 1980), although 10% shallower estimates have also been recorded (Smallwood et al. 1999). The crust thickens to about 25 km at the Hatton Bank on the Rockall Plateau margin (Morgan et al. 1989). For the Greenland-Iceland Ridge, seismic crustal thickness estimates of about 30 km were obtained (Holbrook et al. 2001) that are comparable to gravity estimates (Roman 1999). Seismic crustal thicknesses decrease along the southeastern margin of Greenland from more than 30 km on the Greenland-Iceland Ridge to about 18 km in areas 500-1100 km southeast of this ridge (Holbrook et al. 2001).

Strong interactions between the Iceland Plume and the nearby Mid-Atlantic Ridge system may have formed thickened crust where hotter than normal upper mantle decompresses and melts beneath the ridge. For the Reykjanes Ridge system, 8.5-10 km thick oceanic crust was inferred (Smallwood et al. 1995; 1999; Weir et al. 2001). For the Kolbeinsey Ridge, seismic crustal thicknesses between 7-10 km have been reported (Kodiara et al. 1997).

These disparate results are based on relatively localized investigations and hence are difficult to interpret in the complex regional tectonic framework of this area. However, an effective regional perspective on these seismic and geothermal results can be developed from

crustal thickness estimates obtained from gravity data by spectral correlation analysis (von Frese et al. 1997a) of the terrain gravity effects and free-air gravity anomalies (von Frese et al. 1999).

Specifically, we compare the terrain gravity effects, as computed by Gauss-Legendre quadrature integration (von Frese et al. 1981), to the co-registered free-air gravity anomalies for their correlation spectrum. Spectral correlation filters (von Frese et al. 1997a) are then implemented to extract terrain-correlated and terrain-decorrelated components of the free-air gravity anomalies. By subtracting the terrain-correlated free-air anomalies from the terrain gravity, we isolate the compensated terrain gravity effects assuming the crust is compensated predominantly by its thickness variations. Because the compensated terrain gravity effects are not evident in the ambient free-air gravity field, annihilating gravity effects can be inferred and analysed for mantle relief and crustal thickness variations assuming an appropriate crustal compensation model and effective density contrasts between crust and mantle.

This methodology was developed and validated in crustal studies of the Antarctic (von Frese et al. 1999) and East Asia (Tan & von Frese, 1997), where the estimated Moho was found to be well within 10% of that observed by large offset seismic studies. Similar procedures also were used for crustal analyses of the Moon (Potts 2000) and its Mare Orientale basin (von Frese et al. 1997b, 1998), Venus (Leftwich et al. 1999), Mars (Potts et al. 2002), Greenland (Roman 1999), and Ohio (Kim et al. 2000).

For the present study, we implemented a crust-mantle density contrast grid that accounts for the thermal effects of the Mid-Atlantic Ridge and the Iceland Plume. These thermal effects were estimated from modelling heat flow variations of idealized vertical sheet and cylinder bodies (Simmons 1967).

In the following sections, we describe a comprehensive gravity-based model of the crustal structure of the greater Iceland region. We also compare and contrast our results with seismic refraction models of the crustal structure and thermal regime of the Mid-Atlantic Ridge and Iceland Plume.

2 FREE-AIR GRAVITY ANOMALIES

We calculated free-air gravity anomalies at a 20-km elevation from the spherical harmonic degree and order 360 model EGM96 (Lemoine et al. 1998a; b). Within the study area, the EGM96 coefficients are constrained by mean 30 arc minute anomalies from terrestrial, airborne, and shipborne gravity surveys, as well as satellite altimetry-derived anomalies from data sets compiled by the National Imagery and Mapping Agency (NIMA), NASA's Goddard Space Flight Center, and The Ohio State University. The observational errors of the NIMA free-air anomaly grid, which includes most of the study area, are at most 15 mGal and generally less than 10 mGal with the relatively high-frequency features attenuated at 20 km altitude (Roman 1999).

Fig. 2 shows the free-air gravity anomalies of the Icelandic study region at an altitude of 20 km (Lemoine et al. 1998a; b). A prominent gravity high characterizes the Mid-Atlantic Ridge and extends through western Iceland marking possible mantle upwelling. The distinct gravity maximum over east-central Iceland suggests that the Iceland Plume is situated slightly eastwards of the ridge. The transverse Greenland-Scotland Ridge and Rockall Platform are associated with well defined gravity maxima while the intervening ocean basins are characterized by relative anomaly minima.

3 MODELED TERRAIN GRAVITY EFFECTS

Estimates of the terrain gravity effects are needed to compare with the regional free-air gravity anomalies of the study region. The terrain includes water, ice, and unconsolidated and consolidated rock components. Surface elevations and bathymetry from the JGP95E digital elevation model (DEM) (Smith & Sandwell 1994; 1997) were used for modelling the terrain gravity effects in spherical coordinates by Gauss-Legendre quadrature integration. Roman (1999) found a root-mean-squared (RMS) difference of less than 35 m in comparing JGP95E bathymetric values with 109 control points from independent shipborne soundings in the Barents Sea. In the deeper North Atlantic, regional JGP95E errors up to 2-4 times this RMS value yielded relatively minor terrain gravity errors because of the relatively large

altitude of modelling. Roman (1999) also developed ice thickness estimates for portions of Greenland in the study area from a 6'N × 15'E subglacial DEM obtained from the Danish Cadastre and Survey. The errors in the subglacial topography estimates may approach 500 m, but their effects on our results are also minimal because they are on the periphery of the study area.

Fig. 3 gives the integrated terrain gravity effects of the water, ice, and rock components at an elevation of 20 km. The water and ice effects were modeled for densities of 1020 kg/m^3 and 900 kg/m^3, respectively, while 2800 kg/m^3 was chosen for the rock component. These assumptions and simplifications are sufficient for enhanced modelling of the regional terrain gravity effects because terrain gravity effects are evaluated at altitudes that are large relative to terrain relief where sensitivity for local errors in topographic elevation and density is limited (e.g., von Frese et al. 1999; Kim et al. 2000).

Of course, our density assumptions do not completely account for the complex density variations of the tectonically complicated study region. For example, in new oceanic crust significant local density alterations may result from fractures and faults (e.g., Bjarnason et al. 1993; Flóvenz & Saemundsson 1993). Also, within the crust of Iceland, rocks with higher densities of about 3000 kg/m^3 or greater are common where the Fe and Mg components have been enhanced by the higher plume temperatures (McKenzie 1984; White et al. 1995).

However, errors in our terrain gravity effects may be readily updated as improvements in density information becomes available. For example, in local regions where improved densities may be identified, the differential gravity effects of these regions can be computed using the contrast between the new and old densities and added to our terrain gravity effects to update them.

4 SPECTRAL CORRELATION MODELLING OF THE CRUST

The correlation spectrum (von Frese et al. 1997a) between the Fourier transforms $\boldsymbol{F}$ and $\boldsymbol{T}$ of the free-air gravity anomalies (Fig. 2) and the terrain gravity effects (Fig. 3), respectively, was obtained by:

$$CC(k) = \cos(\Delta\theta_k) = Re\left(\frac{\boldsymbol{F}(k)}{\boldsymbol{T}(k)}\right)\left(\frac{|\boldsymbol{T}(k)|}{|\boldsymbol{F}(k)|}\right), \quad (1)$$

where $CC(k)$ is the correlation coefficient between the kth wavenumber components $\boldsymbol{F}(k)$ and $\boldsymbol{T}(k)$ with amplitude spectra given by $|\boldsymbol{F}(k)|$ and $|\boldsymbol{T}(k)|$, respectively, and Re denotes taking the real parts of the wavenumber components. $CC(k)$ is evaluated from the cosine of the phase difference $(\Delta\theta_k)$ between the two kth wavenumber components. This correlation spectrum depends only on the phase properties between orthogonally gridded and co-registered data sets. Hence Fourier transforms can be used to analyse the two data sets in spherical coordinates for their correlations with absolutely no loss of generality.

From the correlation spectrum, we developed spectral filters to extract the common features in both the free-air anomalies and terrain gravity effects. Specifically, those k-wavenumber components showing positive $(CC_p(k) \geq 0.15)$ and negative $(CC_n(k) \leq -0.22)$ correlations between the free-air anomalies and the terrain effects were identified. These cut-off values for the correlation filter were chosen to minimize correlative features between the terrain-decorrelated free-air and compensated terrain gravity components – i.e., $CC_p(k)$ and $CC_n(k)$ were chosen to give a zero correlation coefficient between the two gravity components that hence could be independently analysed for the properties of the subsurface.

Inversely transforming the correlated free-air wavenumber components yields the terrain-correlated free-air anomalies in Fig. 4 that can constrain the local state of isostatic equilibrium within the context of an appropriate crustal compensation model. Subtracting the terrain-correlated free-air anomalies from the terrain effects yields the compensated terrain gravity effects shown in Fig. 5. Because the compensated terrain effects are not apparent in the free-air anomalies, an annihilating anomaly field can be inferred for interpreting possible Moho relief and crustal thickness variations. Reversing the polarities of the compensated terrain gravity effects yields the gravity effects that annihilate the compensated terrain gravity effects.

These annihilator effects were subjected to least squares inversion for Moho estimates assuming the terrain was compensated by crustal thickness variations. The spherical coor-

dinate Moho model was obtained using Gauss-Legendre quadrature integration to estimate the tops and bottoms of 0.5° × 0.2° prisms about the reference depth of 25 km below sea level. This reference depth, as well as an initial density contrast of 400 kg/m^3 for the mantle relative to the crust, were chosen because they yielded gravity Moho estimates that were well matched with the available seismic Moho depths. However, to maximize the regional correlations with these seismic estimates, the density contrasts across the reference depth were adjusted further to reflect first order thermal variations across the region.

4.1 Regional density variations from thermal models

Heat flow in the North Atlantic is not uniform and decreases sharply away from the axes of the mid-ocean ridge and the Iceland Plume (e.g., Palmáson 1967, 1972, 1974; Langseth et al. 1974, 1990; Flóvenz & Saemundsson, 1993; Pollack et al. 1993). Only the major regional heat flow trends can be identified because these observations show large variability and continuous heat flow mapping comparable to gravity and magnetic surveys is infeasible (e.g., Langseth et al. 1990; Cull & Beardsmore 2001). However, the effects of these lateral variations in mantle temperatures on the density contrasts between the crust and mantle must be considered for effectively modelling regional crustal thickness variations from the gravity data.

For modelling the regional mantle heat flow, we assumed a stabilized thermal regime within the oceanic lithosphere where steady temperatures prevail - i.e., similar thermal conditions exist in equivalent age lithosphere (e.g., Verhoogen 1980; Turcotte & Schubert 1982; Cull & Beardsmore 2001). Experimental studies of free convection suggest that the mantle flow may be sheet-like or laminar beneath the linear morphology of mid-ocean ridges (e.g., Elder 1965; Lenardic & Kaula 1995; Kincaid et al. 1996). A phase change within the upper mantle may have stratified mantle convection and limited upper-lower mantle interactions at the 650 km discontinuity (Schilling 1991; Anderson 1998), thus placing an approximate lower boundary on the mantle flow.

Assuming that the mid-ocean ridge upwellings are laminar, the heat flow entering normal

oceanic lithosphere may be conveniently estimated by the idealized vertical sheet calculation (Simmons 1967). Heat flow entering the oceanic lithosphere from below may exceed 0.100 W/m^2 at the Mid-Atlantic Ridge and decay to about 0.04 W/m^2 for ancient oceanic lithosphere (e.g., Verhoogen 1980; Turcotte & Schubert 1982). For this study, a vertical sheet beneath the Mid-Atlantic Ridge was used to model the effects on Moho density contrasts. The sheet was dimensioned with its bottom at 700 km and its top at 70 km depth within the presumed range of partial melting (McKenzie 1984; Sleep 1996, 1997; Barton & White 1997). The idealized mid-ocean ridge effects were scaled to produce a maximum reduced heat flow of 0.100 W/m^2 beneath the ridge when superposed on an ambient mantle heat flow of 0.04 W/m^2. This mid-ocean ridge modelling performed well with a maximum difference of about 0.02 W/m^2 when tested against ocean heat flow observations and the half space cooling models from Uyeda (1978, 1988), Verhoogen (1980), and Turcotte & Schubert (1982).

We envisioned plume temperatures to decrease from the center of the plume as a Gaussian function (Ito et al. 1996; Wolfe et al. 1997). In the core of the plume beneath Iceland, upper mantle temperatures may reach 1500-1550°C and decrease away from the plume to normal mantle temperatures of about 1300°C. Estimated temperature increases of 200°-250°C are required to generate 15 km of excess crust while a mean mantle temperature of 1350°C can produce oceanic crust of normal thickness (McKenzie 1984). Estimates of 0.130 W/m^2 to over 0.200 W/m^2 have been made for the conductive heat flow entering the lower crust of Iceland over the plume center (Pálmason 1972; Flóvenz & Saemundsson 1993).

The heat flow effects of the idealized vertical cylinder (Simmons 1967) were used to model the mantle plume supplying anomalously hot material to the lithosphere (e.g., Vogt 1974; Sleep 1992, 1997). Geochemical findings infer the lower boundary of mid-ocean ridge convection at the 650 km discontinuity while mantle plumes appear to have deeper sources (Schilling 1991; Sleep 1992; Wolfe et al. 1997). Thinning of the upper mantle transition zone between the 410 km and 660 km discontinuities may reflect plume material that penetrates the transition zone from deeper than 660 km (Shen et al. 1996). Seismic imaging indicates

that the Iceland Plume may extend to the core-mantle boundary (Nataf 2000). For modelling the plume's heat flow, its radius was taken as 75 km, while the depth to its top was set at 70 km within the presumed range of partial melting (McKenzie 1984; Sleep 1996, 1997), and its bottom was placed at infinity.

Fig. 6 gives the superposed plume and ridge heat flow effects from which the density contrasts were scaled. The plume construct is one of a central hot conduit surrounded by relatively warm mantle where temperatures decrease with distance from the plume core. The superposed plume and ridge effects reinforce each other enhancing processes that may propagate geochemical anomalies and elevate thermal conditions far along the ridges and away from the plume.

Our reduced heat flow modelling conforms well to the regional decay of heat flow with distance from the Icelandic Plume and Mid-Atlantic Ridge as shown in Fig. 7. The reduced heat flow is generally less than the surface observations because of the effects of crustal heat production (e.g., Verhoogen, 1980; Turcotte & Schubert 1982; Cull & Beardsmore, 2001). Additional local differences between observed and modeled heat flow values reflect the effects of hydrothermal systems, mid-to-upper crustal magmatic intrusions, and other near-surface thermal conditions that we could ignore in our modelling of the regional mantle heat flow.

We scaled the density contrasts to the combined heat flow effects of the plume and ridge to obtain a density contrast grid of the mantle-crust interface for our Moho inversion. Specifically, a maximum mantle density reduction of 90 kg/m^3 was added to our nominal density contrast of 400 kg/m^3 at the center of the plume to calibrate our gravity estimate to the 39 km depth from seismic Moho sounding (Darbyshire et al. 2000a, b). We lowered this mantle density reduction linearly with the modeled heat flow for a maximum reduction of 40 kg/m^3 at the mid-ocean ridge to zero reductions at the northwestern and southeastern margins of the study area.

Using these spatially variable density contrasts, we obtained Moho estimates that were combined with bathymetric and terrestrial topography data for the crustal thickness model

given in Fig. 8. In the next section, we compare the gravity derived crustal thickness estimates obtained using these density contrasts with the seismic estimates.

5 CRUSTAL STRUCTURE OF THE GREENLAND-SCOTLAND RIDGE

In summary, the crustal thickness model in Fig. 8 was obtained using the above thermally based model for density contrasts across the Moho in the inversion of gravity effects that annihilate the compensated terrain gravity (Fig. 5). Fig. 8 also shows the locations of the seismic control points used in the inversion, as well as coastlines, and the 1,000-m bathymetric contour delineating the Greenland-Scotland Ridge and Rockall Platform. The resulting Moho estimates yielded gravity effects that match more than 99% of the annihilating effects with mean residual of 0.37 mGal to the standard error of 0.09 mGal.

Table 1 compares our gravity Moho estimates with the 21 seismic estimates that are site-coded in Fig. 8. Overall, our gravity Moho estimates have a 0.74 coefficient of correlation with the seismic Moho estimates at the 99% confidence level. Furthermore, the mean difference of the gravity Moho depths relative to the seismic estimates is nearly -1.8 km with the standard error of 1.3 km.

In general, Table 1 suggests the differences in the crustal thickness estimates are greatest for the six [a]-footnoted stations along the Icelandic rift zones and the Mid-Atlantic Ridge where thermal effects and partial melting complicate interpreting both density and seismic velocity variations. On older crust, the differences between seismic and gravity Moho estimates are reduced relative to those on the Kolbeinsey and Reykjanes Ridges and the Krafla volcanic complex. For the remaining 15 control points on relatively mature oceanic crust, the correlation coefficient is 0.81, while the mean difference and its standard error are 1.5 km and 0.5 km, respectively. Clearly, further consideration of the seismic and gravity differences for the younger crust may reveal additional insight on the recent tectonic evolution of the region.

5.1 The crust of Iceland

Uncertainty revolves around the question of whether Iceland has a cool thick or hot thin crust. Some investigations have inferred elevated temperatures and partial melts at shallow depths (e.g., Beblo & Björnsson 1980; Eysteinsson & Hermance 1985; Schmeling 1985; Gudmunsson & Milsom 1997), while recent seismic studies that include reinterpreted and new seismic data suggest a thicker and cooler crust (e.g., Menke & Levin 1994; Staples et al. 1997; Smallwood et al. 1999). For the regions surrounding the plume core and rift zones in eastern and southwestern Iceland, our results are generally consistent with seismic crustal thickness estimates. However, to reconcile the gravity Moho depths with seismic estimates in thermally active regions, anomalous reductions in mantle density are required that may reflect partial melting at shallow depths.

In general, comparing gravity and seismic Moho estimates may help to quantitatively constrain the amount of partial melting in the upper mantle. For example, particularly pronounced discrepancies between gravity and seismic Moho estimates occurred over the Iceland Plume. Here our gravity analysis based on the nominal density contrast of 400 kg/m^3 across the Moho inferred a 45 km deep Moho relative to the 39 km estimate of Darbyshire et al. (1998; 2000a, b) who had invoked mantle density reductions up to 90 kg/m^3 to reconcile their seismic and gravity observations. We require a comparable density reduction to adjust our plume Moho estimate to 39 km. Also, near Krafla beneath the Eastern Rift Zone (**ERZ**), we obtained a Moho depth of roughly 31 km in contrast to the seismic Moho estimate of 20 km obtained by Brandsdóttier et al. (1997) and Staples et al. (1997). These studies also considered gravity Moho estimates that required density reductions for the upper mantle of 70 kg/m^3 and the presence of relatively unconsolidated crust to adjust them to the seismic estimates. Hence, to reconcile the gravity and seismic estimates over the thermally active regions, mantle density reductions of about 70-90 kg/m^3 tend are required.

Thermal inflation of the mantle can only marginally account for the reduction in upper mantle density. For example, for peridotite with a coefficient of volumetric thermal expansion $\alpha_v = 2.5 \times 10^{-5}/°C$ (Turcotte & Schubert 1982; Ravat et al. 1999) and density $\rho =$

3275 kg/m^3, the density reduction ($\delta\rho$) of the mantle due solely to an estimated temperature increase $\delta T = 250$°C is $\delta\rho = -\rho\alpha_v\delta T = -20.5$ kg/m^3. Even the hottest viable plume involving temperature increases up to maybe 400°C higher than ambient mantle temperatures (e.g., McKenzie 1984; Ito et al. 1996) can reduce the density by only 33 kg/m^3. Hence, the density reduction due solely to thermal expansion of mantle material is unlikely to explain the disparate gravity and seismic estimates.

Partial melting in upwelling and decompressing mantle material may well produce an additional reduction of the mantle density. Bott (1965) suggested a 30 kg/m^3 density reduction could result from 10% partial melt in the upper mantle. Magnetotelluric and resistivity studies have inferred high temperatures and 10-20% partial melt at shallow depths within the rift zones (Beblo & Björnsson 1980; Eysteinsson & Hermance 1985; Schmeling 1985). Seismic refraction analysis of the negative Bouguer anomaly of central Iceland ascribes it to density reductions in the upper mantle (Pálmason & Saemundsson 1974). The isentropic upwelling model of McKenzie (1984) predicts upwelling plume material that may meet the solidus at about 60 km with a maximum partial melt component reaching perhaps 20% near the lower crust. Large amounts of partial melt ($\geq$ 5%) also have been estimated by surface wave analysis (Chan et al. 1989), and the analysis of seismic reflection and heat flow data for shallow young (0-5 Ma) asthenosphere of the Iceland Plateau (Sato et al. 1989; Sato & Sacks 1989). Hence, regions of partial melt in the mantle may help account for the disparate gravity and seismic estimates.

To quantify the amount and distribution of partial melting in the upper mantle, various velocity-density relationships may be explored by comparing gravity and seismic data (Ravat et al. 1999). For instance, the ratio of the P wave velocity (V_p) to the solidus velocity for peridotite ($V_{solidus}$ = 7.85 km/s) has been used to infer the percentage of partial melting in the mantle (Sato et al. 1989). Thermal expansion accommodates part of the observed density reduction with an additional 0.15% density reduction for roughly each percent of partial melt (Ravat et al. 1999).

As an example, the density reduction would be only 30 kg/m^3 for peridotite with ρ =

3275 kg/m^3, 2% partial melt reflected by V_p = 7.7 km/s, and 250°C temperature excess. Hence, to produce the 90 kg/m^3 reduction in mantle plume density for the Darbyshire et al. (2000a, b) model, higher temperatures and/or greater percentages of partial melt well in excess of 2% would be required.

Fig. 9 generalizes the percent reduction of mantle density due to thermal expansion and partial melting. The boxed area includes the mantle density reductions inferred for Iceland over the probable ranges of excess plume temperatures (200-400°C) and partial melt components (1-20%). The heavy dashed contours in the box correspond to the 1.85% and 2.77% reductions that decrease the respective mantle densities beneath the rift zones and at the top of the plume by 60 kg/m^3 and 90 kg/m^3, respectively, as required by the Darbyshire et al. (2000a, b) model. We also require comparable density reductions to adjust our gravity Moho estimates at the plume core and rift zones.

The comparison of gravity and seismic Moho estimates also may be limited by the vertical heterogeneity of the Icelandic crust. Large variations in surface heat flow (Fig. 7) within Icelandic neovolcanic zones suggest the crust may be laterally and vertically intruded. Evidence for these regions being compositionally and structurally differentiated is suggested by exposed intrusions such as the complexly layered Oman Ophiolite (Korenaga & Kelemen 1997) and the Skaergaard complexes (Nielsen & Brooks 1995; Andersen et al. 1998). Deeply eroded Icelandic volcanoes reveal numerous crustal complexities such as the Austurhorn intrusion where competent basalts and gabbros were interleaved with magma (Blake 1966; Åberg et al. 1987). Hence, seismic Moho estimates may reflect the complicated effects of seismically competent mafic components interbedded with relatively acidic, less competent and dense units containing partial melts in the upper mantle and lower crust of Iceland. The presence of smaller scale melt fractions can also significantly complicate seismic interpretation (Hammond & Humphreys 2000; Takei 2002).

However, despite the uncertainties regarding the geometries of small-scale melt fractions, the regional trend of increasing *P*-to-*S* wave velocity ratios (V_p/V_s) towards the plume tends to support partial melting near its core (Darbyshire et al. 2000a; Hammond & Humphreys

2000). Estimates for partially molten upper mantle containing over 1% partial melt indicate P and S wave velocity reductions per percent melt of at least 3.6% and 7.9%, respectively (Hammond & Humphreys 2000). Hence (V_p/V_s)-values in excess of roughly 1.67 may reflect the presence of partial melt fractions.

For much of eastern Iceland, (V_p/V_s)-values ranging around 1.76-1.79 suggest near-melting temperatures (Brandsdóttier et al. 1997). However, north of the Krafla volcanic complex, a $V_p/V_s = 1.88$ may indicate an apparent increase in temperatures in the lower crust towards the rift zone (Darbyshire et al. 2000a).

These increasing V_p/V_s gradients towards the plume center and rift zones are also consistent with our thermal modelling that infers great lateral thermal variability beneath Iceland. Temperatures may approach the basalt solidus at shallow depths above the plume core, but fall off sharply away from the plume and rift zones, which can help channel plume material along the diverging boundary (Sleep 1997).

Depth variations in the 1200°C basalt solidus may be calculated from heat flow estimates by *Fourier's* temperature equation (Turcotte & Schubert 1982; Fowler 1992; Cull & Beardsmore 2001). Heat flow values associated with Iceland's geothermal areas within the rift zones can exceed 0.4 W/m^3 to reflect higher order effects of mid- to upper-crustal intrusions, magma bodies, and circulating hydrothermal fluids within the crust (Palmáson, 1967; 1972; 1974). Crustal temperatures may be inferred assuming a modest reduced heat flow effect of 0.150 W/m^2 for the superposed plume and ridge system and a crustal thermal conductivity of 2.0 W/m^3K and heat production of $300\times10^{-12}W/m^3$ (Flóvenz & Saemundsson 1993). These conservative estimates indicate the basalt solidus may be as shallow as 18 km directly above the plume but deepens sharply away from its core as shown by the crustal profile in Fig. 10.

Beneath Iceland, the inferred lateral temperature gradients can help explain apparently conflicting regional crustal models in terms of possible mantle regions of partial melt. Seismically competent mantle and crust interbedded with less competent and dense units containing partial melts above the plume core may account for the differences between our crustal

thickness estimates and seismic estimates and earlier magnetotelluric, resistivity, seismic, and thermal crustal thickness estimates. For example, in southwestern Iceland Bjarnason et al. (1993) found a 20-25 km thick crust with a seismic Moho that was discontinuous across the Western Rift Zone. Beneath the **WRZ**, we inferred Moho at roughly 33 km, while Bransdóttir et al. (1997) have interpreted a 19 km deep Moho at a broad doming of high velocity material derived possibly from magma in the lower crust. At the **ERZ** near the Krafla volcanic complex, Bransdóttir et al. (1997) and Staples et al. (1997) inferred seismic Moho at about 20-25 km compared to our estimates of 25-33 km.

These discrepancies may reflect a mantle region of partial melt that feeds mid-to-upper crustal magma chambers through systems of listric faults and rifts of the neovolcanic zones. By our thermal modelling, partial melts may extend to about 20 km or less above the plume core and rift zones (Fig. 10) that help channel plume material along the diverging plate boundary. This partial melt region may also feed cumulate layers that underplate the diverging oceanic crust (Pálmason 1980).

To account for both the extension of enhanced crustal thickness and geochemical anomalies for hundreds of kilometers about the plume, models of plume-ridge interactions commonly imply the intersection of laterally spreading sub-lithospheric plume material (e.g., Vogt 1971; Kincaid et al. 1995; Ito et al. 1996; Ribe et al. 1995, 1996; Sleep, 1996, 1997). Enhanced flow of plume material may occur along the axes of nearby ocean ridges (e.g., Schilling 1991; Sleep 1996). Additionally, drag on the plume material from the overlying spreading lithospheric plates may promote the flow of plume material across the ridge axis as it migrates away from the plume. This flow of plume material may be enhanced under the slower moving trailing plate with reduced drag, while for the leading plate it would be reduced in the direction of relative plume migration (Ito et al. 1997).

Our crustal thickness estimates may also reflect density reductions associated with hotter, less viscous material, which may propagate along Iceland's rift zones. Hence the flow of plume material is consistent with thickened crust in Fig. 8 that extends along the active Eastern Rift Zone, towards western Iceland and north towards the Kolbeinsey Ridge and southwards

down the Reykjanes Peninsula. The apparent dispersion of plume material can be correlated to the rift zones and the active volcanic regions of Iceland.

On a regional basis, thickened crust is most prominent from southeastern Greenland to Iceland where it appears to truncate at the leading edge of the European Plate and elongates along the trailing North American margin. These results are consistent with the Late Tertiary path of the North American Plate across the Iceland Plume where lithospheric drag enhanced the dispersion of plume material on the trailing lithospheric plate and retarded it on the leading plate (Ito et al. 1997). Hence, our gravity crustal model may help illuminate plume material that was channeled westward with the trailing lithospheric plate, as well as along the rift zones beneath Iceland.

5.2 Tertiary plume-ridge interaction

Sea-floor spreading in the northeastern Atlantic was accompanied by the upwelling of anomalously hot asthenosphere along 2000 km of rifted margin between northwestern Europe and Greenland that was followed by an apparent decay of the mantle thermal anomaly (Barton & White 1997). Radiometric dating of Tertiary igneous units in East Greenland and at the Vøring margins in Norway indicate the commencement of rifting and flood basalt volcanism by about 55 Ma (Bott & Gunnarsson 1980; White et al. 1992; Price et al. 1997; Barton & White 1997; Sleep 1997). The volume of these extrusions may have been as great as 10 million km^3 (White & McKenzie 1989). These results suggest that rifting and sea-floor spreading in the North Atlantic began in the proximity of a nascent plume head (White & McKenzie 1989; Sleep 1997). However, other studies suggest that the Iceland Plume was beneath Greenland when sea-floor spreading began so that it may predate North Atlantic rifting (Morgan 1983; Vink 1984; Lawver & Müller 1994; Brozena 1995).

The Greenland and Scotland portions of the Greenland-Scotland Ridge reflect somewhat different developmental histories. The Iceland-Faeroe ridge developed between 55 and 30 Ma as a subaerial volcanic plateau (Fleischer et al. 1974; Nilsen 1983). By 36 Ma, most of the Iceland-Faeroe portion of the Greenland-Scotland Ridge had probably formed (Vink 1984).

The continental Jan Mayen Block was rifted off East Greenland as active plate divergence began shifting from the Aegir Ridge north of the Iceland-Faeroe Ridge to the incipient Kolbeinsey Ridge at roughly 36 Ma. This shift of the ridge axis may have occurred when the Iceland Plume emerged from beneath Greenland's continental lithosphere (Nunns 1983; Vink 1984). Sea-floor spreading possibly continued on both the Aegir and the Kolbeinsey Ridges until about 20 Ma as the Iceland Plume migrated eastwards relative to the spreading ridge.

The Iceland Plume interacted strongly with the Mid-Atlantic Ridge system, producing thickened oceanic crust as the hotter than normal upper mantle decompressed beneath the spreading axis (Mckenzie 1984; White et al. 1992; Smallwood et al. 1995). Plume enhanced crustal thickening can be seen in Fig. 8 to extend some 400-500 km from the transverse Greenland-Scotland Ridge axis. This result agrees with predictions that near-ridge plumes influence mid-ocean upwelling temperatures and chemistry to perhaps hundreds of kilometers (Sleep 1997). Seismic experiments also show that thickened oceanic crust was produced relatively far away from the Iceland Plume (Smallwood et al. 1995, 1999; Barton & White 1997; Kodiara et al. 1997; Weir et al. 2001). Geochemical analyses indicate the plume's effects may extend along the Mid-Atlantic Ridge for perhaps a 1000 km or more (Schilling 1991, 1999; White et al. 1995; Fitton et al. 1997; Peate et al. 2001). Our modeled superposition of the thermal effects of the mantle plume and upwelling mid-ocean ridge also suggest enhanced thermal conditions that extend north and south for more than 500 km along the northeastern Mid-Atlantic Ridge.

Our crustal thickness estimates for the Greenland-Iceland Ridge are increased by 3-5 km relative to the Iceland-Faeroe Ridge. This result may reflect the relative east-to-west migration of the North Atlantic crust and Mid-Atlantic Ridge over the Iceland Plume. Volcanism and underplating may have emplaced additional crust into the Greenland-Iceland Ridge as the oceanic crust passed over the plume. Hence, the thickened crust that stretches across the Greenland-Iceland Ridge to western Iceland may reflect the hotspot trace.

Eastward shifts in Iceland's rift axes also reflect a relatively northwesterly trajectory for

lithosphere overlying the Iceland Plume. The Iceland Plateau was created by ridge-centered and near-ridge hotspot magmatism and volcanism with maximum volcanic ages of 16 Ma that generally decrease towards the rift zones (Jancin et al. 1985). The Mid-Atlantic Ridge apparently overrode the Iceland hotspot from the east and continues to move westwards relative to the hotspot, but is accommodated by shifts in rifting to the east (Oskarsson et al., 1985). Stratigraphic analysis and radiometric dating of the active Eastern and Western Rift Zones indicate a recent overall eastward shift of rifting in Iceland at about 6-7 Ma (Jancin et al. 1985). Crustal accretion from multiple zones in northern Iceland was shifted to the northeastern axial rift zone with a concurrent eastward shift of rifting in the south as the lithosphere continued drifting westwards above the Iceland Plume. In Fig. 8, the plume's path beneath Iceland may be indicated by thick crust in excess of 30 km that stretches westwards across the Iceland Plateau.

6 CONCLUSIONS

Spectral correlations between free-air gravity anomalies and terrain gravity effects provide new regional perspectives for considering the tectonic significance of more local geological, seismic, geothermal, and other geophysical observations. Spectral correlation modelling of the crust associated with Iceland and the Greenland-Scotland Ridge agrees with and extends the crustal results of the disparate geophysical investigations.

Our study confirms the presence of thickened crust for hundreds of kilometers across the transverse ridge. For the Iceland Plume, crustal thickening is most pronounced over its core and decays sharply towards its margin. However, the gravity modelling of crustal thickness can be enhanced by taking into account density effects due to thermal expansion and partial melting via the regional thermal regime modeled by superposition of an idealized thermal plume and mid-ocean ridge.

Our results suggest that the Greenland-Iceland Ridge crust is thicker than crust for the Iceland-Faeroe Ridge. Additional crust may have been emplaced on the Greenland-Iceland Ridge as the Mid-Atlantic Ridge overrode the plume from the east. Thickened crust in Fig.

8 stretching along the Greenland-Iceland Ridge and eastwards across the Iceland Plateau may trace the path of the plume to its inferred location roughly beneath Grímsvötn (64.6°N, 17.4°W) and the Vatnajökull glacier where it is closely associated with the central Icelandic volcanoes and neovolcanic zones.

Disparities between the seismic and gravity Moho estimates occur for the Icelandic neovolcanic zones and at the Reykjanes and Kolbeinsey Ridges. These relatively deeper gravity Moho estimates may reflect lower density regions of the upper mantle that for the plume may include an 8-20% partial melt component. Hence, our results may help illuminate the partial melt regions that feed the neovolcanic zones and the cumulates at the base of the diverging lithosphere.

Newly available satellite geopotential observations from the low-Earth orbiting Ørsted, CHAMP, and GRACE missions (e.g., von Frese et al. 2000) may well give additional perspectives on the crustal tectonics of the Icelandic study region. Satellite magnetic and gravity observations provide new and important boundary conditions for crustal analyses of near-surface and surface geopotential surveys and other goephysical data. For the tectonically active Icelandic study region in particular, the satellite geopotential field observations can facilitate the regional synthesis of the disparate heat flow data because of the effects of temperature on crustal density and magnetization (e.g., Leftwich et al. 2000; von Frese et al. 2000).

ACKNOWLEDGMENTS

Elements of this research were supported by grants from NASA (NAG5-7645), and the Department of Geological Sciences, Ohio Supercomputer Center, Center for Mapping, and Laboratory for Space Geodesy and Remote Sensing Research at The Ohio State University. This paper was also presented at The Symposium on the Icelandic Plume and Crust with the support of the National Science Foundation, Iceland Research Council, US Ridge Office, and Svartsengi Geothermal Power Plant.

REFERENCES

Åberg, G., Bollman, B., and R. M. Macintyre, 1987, Age of the Austurhorn intrusion: A net-veined complex in southeastern Iceland, *GFF Lit. Rev., 109,* 291 - 294.

Andersen, J. C. O., T. F. D. Nielsen, J. G. Rønsbo, The Triple Group and the Platinova Gold and Palladium Reefs in the Skaergaard Intrusion: Stratigraphic and petrographic relations, *Economic Geology, 93,* 488 - 509, 1998.

Anderson, D. L., 1998, The scales of mantle convection, *Tectonophysics, 284,* 1 - 17.

Barton, A. J., and R. S. White, 1997, Crustal structure of the Edoras Bank continental margin and mantle thermal anomalies beneath the North Atlantic, *J. Geophys. Res., 102,* 3109 - 3129.

Beblo, M., and A. Bjornsson, 1980, A model of electrical resistivity beneath NE-Iceland: Correlation with temperature, *J. Geophys., 47,* 184-190.

Bjarnason, I., Th., and Menke, W., Flovenz, O. G., Caress, D., 1993, Tomographic image of the Mid-Atlantic plate boundary in Southwestern Iceland, *J. Geophys. Res., 98,* 6607 - 6622.

Bjornsson, S., 1983, Crust and upper mantle beneath Iceland, in *Structure and Development of the Greenland-Scotland Ridge,* edited by M. H. P. Bott, S. Saxov, M. Talwani, and J. Thiede, Plenum Press, New York, 31 - 61.

Blake, D. H., 1966, The net-veined complex of the Austerhorn Intrusion, Southeastern Iceland *J. Geol., 74,* 891 - 895.

Bott, M. H. P., 1965, The upper mantle beneath Iceland, *Geophys. J. Roy. Astron. Soc., 8,* 275 - 277.

Bott, M. H. P., and K. Gunnarsson, 1980, Crustal structure of the Iceland-Faeroe Ridge, *J. Geophys., 47,* 221 - 227.

Bransdóttir, B., W. Menke, P. Einarsson, R. S. White, R. K. Staples, 1997, Färoe-Iceland Ridge Experiment 2. Crustal structure of the Krafla central volcano, *J. Geophys. Res., 102,* 7867 - 7886.

Breivick, A. J., J. Verhoef, J. I. Faleide, 1999, Effect of thermal contrasts on gravity modeling at passive margins: Results from the western Barents Sea, *J. Geophys. Res., 104,* 15293 - 15311.

Brozena, J. M. 1995, Kinematic GPS and Aerogeophysical Measurement: Gravity, Topography, and Magnetics, Ph.D. Dissertation, *University of Cambridge.*

Chan, W. W. and I. S. Sacks, 1989, R. Morrow, Anelasticity of the Iceland Plateau from surface wave analysis, *J. Geophys. Res., 94,* 5675 - 6588.

Cull, J. P., and G. R. Beardsmore, 2001, Crustal Heat Flow: A Guide to Measurement and Modeling, Cambridge University Press, Cambridge, 324 pp..

Darbyshire, I. Bjarnason, F. A., R. S. White, and O. G. Flovenz, 1998, Crustal structure above the Iceland mantle plume: Images by the ICEMELT experiment, *Geopys. J. Int., 135,* 1131 - 1149.

Darbyshire, F. A., R. S. White, K. F. Priestley, 2000a, Structure of the crust and uppermost mantle of Iceland from a combined seismic and gravity survey, *Earth Planet. Sci. Lett., 181,* 409 - 428.

Darbyshire, F. A., K. F. Priestley, R. S. White, R. Stefánsson, G. B. Gudmundsson, S. S. Jakobsdóttir, 2000b, Crustal structure of central and northern Iceland from analysis of teleseismic receiver functions, *Geophys. J. Int., 143,* 163 - 184.

Elder, J. W., 1965, Physical processes in geothermal areas in *Terrestrial Heat Flow,* edited by W. H. K. Lee, pp. 211 - 239, AGU Geophysical Monogram 8, Washington.

Eysteinsson, H., and Hermance, J. F., 1985, Magnetotelluric measurements across the eastern neovolcanic zone in south Iceland, *J. Geophys. Res., 90,* 10093 - 10103.

Fitton, J. G., A. D. Saunders, M. J. Norry, B. S. Hardarson, R. N.Taylor., 1997, Thermal and chemical structure of the Iceland plume, *Earth Planet. Sci. Lett., 153,* 197 - 208.

Fleischer, U., Holzkamm, F., Vollbrecht, K., Voppel, D., 1974, Die Strucktur des Island-Färöer-Ruckens aus geophysikalischen Messungen, *Sonderdruck aus der Deutschen Hydrographischen Zeitschrift, 27,* 97 - 113.

Flóvenz, O., G., and Saemundsson, K., 1993, Heat flow and geothermal processes in Iceland, *Tectonophysics, 225,* 123 - 138.

Fowler, C. M. R., 1996, *The Solid Earth: An Intruduction to Global Geophysics,* pp 176 - 179, New York: Cambridge Univ. Press..

Gudmundsson, M. G., and J. Milsom, 1997, Gravity and magnetic studies of subglacial Grimsvötn volcano, Iceland: Implications for crustal and thermal structure *J. Geophys. Res., 102,* 7691 - 7704.

Hammond, W. C., and E. D. Humphreys, 2000, Upper mantle seismic wave velocity: Effects of realistic partial melt geometries, *J. Geophys. Res., 105,* 10975 - 10986.

Holbrook, W. S., H. C. Larsen, J. Korenaga, T. Dahl-Jensen, I. D. Reid, P. B. Kelemen, J. R. Hopper, G. M. Kent, D. Lizarralde, S. Bernstein, R. S. Detrick, 2001, Mantle thermal structure and active upwelling during continental breakup in the North Atlantic, *Earth Planet. Sci. Lett., 190,* 251 - 266.

Ito, G., J. Lin, 1995, Oceanic spreading center-hotspot interactions: Constraints from along-isochron bathymetric and gravity anomalies, *Geology, 23,* 657 - 660.

Ito, G., Lin, J., Gable., Carl W., 1996, Dynamics of mantle flow and melting at a ridge-centered hotspot: Iceland and the Mid-Atlantic Ridge, *Earth Planet. Sci. Lett., 144,* 53 - 74.

Ito, G., Lin, J., Gable., Carl W., Interaction of mantle plumes and migrating mid-ocean ridges: Implications for the Galapágos plume-ridge system, *J. Geophys. Res., 102,* 15403 - 15417, 1997.

Jancin, M., Young, K. D., Voight, B., Aronson, J. L., Saemundsson, K., Stratigraphy and K/Ar ages across the west flank of the Northeast Iceland Axial Rift Zone in relation to the 7 Ma

volcano-tectonic reorganization of Iceland, *J. Geophys. Res., 90,* 9961 - 9985, 1985.

Kim, J. W., R. R. B. von Frese, and H. R. Kim, Crustal modeling from spectrally correlated free-air and terrain gravity data–A case study of Ohio, *Geophysics, 65,* 1057 - 1069, 2000.

Kincaid, C., G. Ito, and C. Gable, Laboratory investigation of the interaction of off-axis mantle plumes and spreading centers, *Nature, 376,* 758 - 761, 1995.

Kincaid, C., D. W. Sparks, R. Detrick, 1996, The relative importance of plate-driven and buoyancy-driven flow at mid-ocean ridges, *J. Geophys. Res., 101,* 16177 - 16193.

Kodaira, S., K. Gunnarsson, R. Mjelde, H. Shimamura, H. Shiobara, 1997, Crustal structure of the Kolbeinsey Ridge, North Atlantic, obtained by use of ocean bottom seismographs, *J. Geophys. Res., 102,* 3131 - 3151.

Korenaga, J., P. Kelemen, 1997, Origin of gabbro sills in the Moho transition zone of the Oman Ophiolite: Implications for magma transport in the oceanic lower crust, *J. Geophys. Res., 102,* 27729 - 27749.

Langseth, M. G., and G. W. Zielinski, 1974, Marine heat flow measurements in the Norwegian-Greenland Sea and in the vicinity of Iceland, in *Geodynamics of Iceland and the North Atlantic Area,* ed., L. Kristjansson, D. Reidel Publishing Company., Dordrecht-Holland, 277 - 295.

Langseth, M. G., A. H. Lachenbruch, and B. V. Marshall, 1990, Geothermal observations in the Arctic region, in *The Geology of North America Vol., L.,* edited by A. Grantz, L. Johnson, J. F. Sweeney, *The Arctic Ocean region The Geological Society of America,* pp.133 - 151.

Lawver, L. A. and R. D. Müller, 1994, Iceland hotspot track, *Geology,* 22, 311 - 314.

Leftwich, T. E., R. R. B. von Frese, H. R. Kim, H. C. Noltimier, L. V. Potts, D. R. Roman, and L. Tan, 1999, Crustal analysis of Venus from Magellan satellite observations at Atalanta Planitia, Beta Regio, and Thetis Regio, *J. Geophys. Res., 104,* 8441 - 8462.

Leftwich, T. E., H. R. Kim , R. R. B. von Frese, 2000, Geopotential constraints on the crustal structure of the Greenland-Scotland Ridge (abstract), *EOS Trans. AGU, Spring Meet. Suppl., 81 (19),* S175.

Lemoine, F. G., D. S. Chinn, S. M. Cox, J.K. Factor, S. C. Kenyon, S. M. Klosko, S. B. Luthcke, T. R. Olson, E. C. Pavlis,N. K. Pavlis, R. H. Rapp, M. H. Torrence, R. G. Trimmer, Y. M. Wang, Y. M.; R. G. Williamson, 1998a, The Development of the joint NASA GSFC and the National Imagery and Mapping Agency (NIMA) Geopotential Model EGM96, National Aeronautics and Space Administration (NASA), Scientific and Technical Information Office, *NASA Technical Paper 0148-8341 ; NASA/TP-1998-206861.*

Lemoine, F. G., D. S. Chinn, S. M. Cox, R. Dietrich, 1998b, Gravity field improvement activities at NASA GSFC, in *International Association of Geodesy Symposia., 119,* ed. Feissel Martine, 92 - 96, Springer-Verlag, New York.

Lenardic, A., and W. M. Kaula, 1995, Mantle dynamics and the heat flow into the Earth's continents, *Nature, 378,* 709 - 711.

McKenzie, D, 1984, The generation and compaction of partially molten rock, *Journ. Pet, 25,* 713 - 765.

Menke, W. and Levin, V., 1994, Cold crust in a hot spot, *Geophys. Res. Lett., 385,* 1967 - 1970.

Menke, W., 1999, Crustal isostasy indicates anomalous densities beneath Iceland *Geophys. Res. Lett., 26,* 1215 - 1218.

Morgan, W. J., 1983, Hotspot tracks and the early rifting of the Atlantic, *Tectonophysics,* 94, 123 - 139.

Morgan, J. V., P. J. Barton, R. S. White, 1989, The Hatton Bank continental margin–III. Structure from wide-angle OBS and multichannel seismic refraction profiles, *Geophys. J. Int., 98,* 367 - 384.

Nataf, H-C., 2000, Seismic imaging of mantle plumes, *Annu. Rev. Earth Planet. Sci., 28,* 391 - 417.

Nielsen, T. F. D., and C. K. Brooks, 1995, Precious metals in magmas of East Greenland: Factors important to the mineralization in the Skaergaard Intrusion, *Economic Geology, 90,* 1911 - 1917.

Nilsen, T. H., 1983, Influence of the Greenland-Scotland Ridge on the geological history of the North Atlantic and Norwegian-Greenland Sea areas, in *Structure and Development of the Greenland-Scotland Ridge,* edited by M. H. P. Bott, S. Saxov, M. Talwani, and J. Thiede, Plenum Press, New York, 457 - 478.

Nunns, A. G., 1983, Plate tectonic evolution of the Greenland-Scotland Ridge and surrounding regions in *Structure and Development of the Greenlin* Structure and Development of the Greenland-Scotland Ridge, *and-Scotland Ridge,* edited by M. H. P. Bott, S. Saxov, M. Talwani, and J. Thiede, Plenum Press, New York, 11 - 30.

Oskarsson, N., Steinthorsson, S., Sigvaldason, G. E., 1985, Iceland geochemical anomaly: Origin, volcanotectonics, chemical fractionation and isotope evolution of the crust, *J. Geophys. Res., 90,* 10011 - 10025.

Pálmason, G., 1967, On heat flow in Iceland in relation to the Mid-Atlantic Ridge, in *Iceland and the Mid-Ocean Ridges,* edited by S. Björnsson, pp. 111 - 127.

Pálmason, G., 1972, Kinematics and heat flow in a volcanic rift zone, with application to Iceland, *Geophys. J. R. astr. Soc., 33,* 451 - 481.

Pálmason, G., 1974, Heat flow and hydrothermal activity in Iceland, in *Geodynamics of Iceland and the North Atlantic Area,* ed., L. Kristjansson, D. Reidel Publishing Company., Dordrecht-Holland, 297 - 306.

Pálmason, G., and K. Saemundsson, 1974, Iceland in relation to the Mid-Atlantic Ridge, *Annual*

Rev. Earth Planet. Sci., 2, 25 - 50.

Pálmason, G., 1980, A continuum model of crustal generation in Iceland: Kinematic aspects, *J. Geophys., 47,* 7 - 18.

Peate D. W., C. J. Hawkesworth, P. W., van Calsteren, R. N. Taylor, B. J. Murton, 1977, ^{238}U-^{230}Th constraints on mantle upwelling and plume-ridge interaction along the Reykjanes Ridge, *Earth Planet. Sci. Lett., 187,* no. 3-4, 259 - 272, 2001 in *Structure and Development of the Greenland-Scotland Ridge,*

Potts, Laramie V., 2000, Satellite Geophysical Investigations of the Moon, Ph.D. Dissertation, *The Ohio State University,.*

Potts, L . V. , R. R. von Frese and C. K. Shum, 2002, Crustal properties of Mercury from a morphometric analysis of multi-ring basins on the Moon and Mars, *Meteoritics and Planetary Science 37,* 1197-1207.

Price, S., Brodie, J., Witham, A., Kent, R., 1997, Mid-Tertiary rifting and magmatism in the Traill Ø region, East Greenland, *J. Geol. Soc. Lon., 155,* 419 - 434.

Ravat, D., Z. Lu, L. W. Braile, 1999, Velocity-density relationships and modeling the lithospheric density variations of the Kenya Rift, *Tectonophysics, 302,* 225 - 240.

Ribe, N. M., U. R. Christensen, J. Theißing, 1995, The dynamics of plume-ridge interaction, 1; Ridge-centered plumes, *Earth Planet. Sci. Lett., 134,* 155 - 168.

Ribe, N. M., 1996, The dynamics of plume-ridge interaction 2. Off-ridge plumes, J. Geophys. Rev., 101, 16195 - 16204.

Roman, Daniel R., 1999, An Integrated Geophysical Investigation of Greenland's Tectonic History, Ph.D. Dissertation, *The Ohio State University,.*

Sato, H., I. S. Sacks, T. Murase, 1989, The use of laboratory velocity data for estimating temperature and partial melt fraction in the low-velocity zone: Comparison with heat flow and electrical conductivity studies, *J. Geophys. Rev., 94,* 5689 - 5704.

Sato, H. and I. S. Sacks, 1989, Anelasticity and thermal structure of the oceanic upper mantle: Temperature calibration with heat flow data, *J. Geophys. Rev., 94,* 5705 - 5715.

Schilling, J., 1991, Fluxes and excess temperatures of mantle plumes inferred from their interaction with migrating mid-ocean ridges, *Nature, 352,* 397 - 403.

Schilling, J. G., D. Kingsley, D. Fontignie, R. Poreda, and S. Xue, 1999, Dispersion of the Jan Mayan and the Iceland mantle plumes in the Arctic: A He-Pb-Nd-Sr isotope tracer study of basalts from the Kolbeinsey, Mohns, and Knipovich Ridges, *J. Geophys. Res., 104,* 10543 - 10569.

Schmeling, H., 1985, Partial melt below Iceland: A combined interpretation of seismic and conductivity data, *J. Geophys. Res., 90,* 10105 - 10116.

Shen, Y., S. C. Solomon, I. Th. Bjarnason, and G. M. Purdy, 1996, Hot mantle transition zone beneath Iceland and the adjacent Mid-Atlantic Ridge inferred from P-to-S conversion at the 410- and 660-km discontinuities, *Geophys. Res. Lett. 23,* 3527 - 3530.

Simmons, G., 1967, Interpretations of heat flow anomalies, *Rev. of Geophys., 5,* 43 - 52.

Sleep, N. H., 1990, Hotpots and mantle plumes: Some phenomenology, *J. Geophys. Res. 95,* 6715 - 6736.

Sleep, N. H., 1992, Time dependence of mantle plumes: Some simple theory, *J. Geophys. Res., 97,* 20007 - 20019.

Sleep, N. H., 1996, Lateral flow of hot plume material ponded at sublithospheric depths, *J. Geophys. Res., 101,* 28065 - 28083.

Sleep, N. H., 1997, Lateral flow and ponding of starting plume material, *J. Geophys. Res., 102,* 10001 - 10012.

Smallwood, J. R., R. S. White, T. A. Minshull, 1995, Sea-floor spreading in the presence of the Iceland Plume: The structure of the Reykjanes Ridge at 61°40'N, *J. Geol. Soc. Lon., 152,* 1023 - 1029.

Smallwood, J. R., R. K. Staples, K. R. Richardson, , R. S. White, 1999, Crust generated above the Iceland mantle plume: From continental rift to oceanic spreading center, *J. Geophys. Res., 104,* 22885 - 22902.

Smith, W. H. F, and D. T. Sandwell, 1994, Bathymetric prediction from dense satellite altimetry and sparse shipboard bathymetry, *J. Geopys. Res., 99,* 21803 - 21824.

Smith, W. H. F, and D. T. Sandwell, 1997, Global sea floor topography from satellite altimetry and ship depth soundings, *Science, 277,* 1956 - 1962.

Staples, R. K., R. S. White, B. Brandsdóttier, W. Menke, P. K. H. McGuire, J. H. McBride, 1997, Färoe-Iceland Ridge Experiment 1: Crustal structure of northeastern Iceland, *J. Geophys. Res., 102,* 7849-7866.

Takei, Y., 2002, Effect of pore geometry on V_p/V_s: From equilibrium geometry to crack, *J. Geophys. Res., 107,* 10.1029/2001JB000522.

Tan, L., and R. R. B. von Frese, 1997, Satellite geopotential models of the East Asian lithosphere (abstract), *Trans. AGU, 78,* Spring Meet. Suppl., 114.

Turcotte, D. L. and G. Schubert, 1982, *Geodynamics* 450 pp. John Wiley, New York.

Uyeda, S., and D. M. Hussong, 1978, General results of DSDP Leg 60, the eastern portion of the South Philippine Sea transect along 18 degrees N, *Eos, 59,* 1179 Washington.

Uyeda, S. D., 1988, Implications, in *Handbook of Terrestrial Heat Flow Determinations,* edited by R. Haenel, L. Rybach, and L. Stegena, *Kluwer Academic Publishers,* Dordrecht-Holland, 317 - 351.

Verhoogen, J., 1980, *Energetics of the Earth,* 139 pp. National Academy of Sciences, Washington.

Vink, G. E., 1984, A hotspot model for Iceland and the Vøring Plateau, *J. Geopyhys., 89,* 9949 - 9959.

Vogt, P. R., 1971, Asthenosphere motion recorded by the ocean floor south of Iceland, *Earth Planet. Sci. Lett., 13,* 153 - 160.

Vogt, P. R., 1974, The Iceland phenomenon: Imprints of a hot spot on the ocean crust, and implications for the flow below the plates, in *Geodynamics of Iceland and the North Atlantic Area,* ed., L. Kristjansson, D. Reidel Publishing Company., Dordrecht-Holland, 105 - 126.

von Frese, R. R. B., W. J. Hinze, L. W. Braile, and A. J. Luca, 1981, Spherical Earth gravity and magnetic anomaly modeling by Gauss-Legendre quadrature integration, *J. Geopyhys., 49,* 234 - 242.

von Frese, R. R. B., M. B. Jones, J. W. Kim, and J. H. Kim, 1997a, Analysis of anomaly correlations, *Geopyhysics., 62,* 234 - 242.

von Frese, R. R. B, L. Tan, L.V Potts, J.W. Kim, C. J. Merry, and J. D. Bossler, 1997b, Lunar crustal analysis of Mare Orientale from topographic and gravity correlations, *J. Geophys. Res., 102,* 25657 - 25676.

von Frese, R. R. B., L. V. Potts, L. Tan, J. W. Kim, T. E. Leftwich, C. J. Merry, and J. D. Bossler, 1998, Comparative crustal modeling of the Moon and Earth from topographic and gravity correlations, (abstract 1870) *Lunar and Planet. Sci. XXIX,* [CD-ROM].

von Frese, R. R. B., L. Tan, J. W. Kim, and C. R. Bentley, 1999, Antarctic crustal modeling from spectrally correlated free-air and terrain gravity data, *J. Geophys. Res., 104* 25275 - 25296.

von Frese, R. R. B., H. R. Kim, T. E. Leftwich, and J. W. Kim, 2000, Ørsted magnetometer constraints on the crustal structure of the Greenland-Scotland Ridge, in *Proceedings, 3rd Ørsted International Science Team Meeting,* edited by T. Neubert and P. Ultré-Guérard, Danish Meteorological Institute, Tech. Rept. 00-22, ISSN-0906-897x, 4pp.

White, R. S, and D. McKenzie, 1989, Magmatism at rift zones: The generation of volcanic continental margins and flood basalts, *J. Geophys. Res., 94,* 7685 - 7729.

White, R. S, D. McKenzie, R. K., O'Nions, 1992, Oceanic crustal thicknesses from seismic measurments and rare earth element inversions, *J. Geophys. Res., 97,* 19683 - 19715.

White, R. S., J. W., Brown, J. R., Smallwood, 1995, The temperature of the Iceland plume and origin of outward-propagating V-shaped ridges, *Nature, 385,* 245 - 247.

Weir, N. R. W., R. S. White, B. Brandsdóttir, P. Einarsson, H. Shimamura, H. Shiobara, 1998, Crustal structure of the Mid-Atlantic Ridge: The Reykjanes Ridge Iceland Seismic Experiment *(Abs), EOS Trans. AGU 1998 Fall Meeting Suppl.,* F805.

Weir, N. R. W., R. S. White, B. Brandsdóttir, P. Einarsson, H. Shimamura, H. Shiobara, and the

RISE Fieldwork Team, 2001, Crustal structure of the northern Reykjanes Ridge and Reykjanes Peninsula, southwest Iceland *J. Geophys. Res., 106*, 6347 - 6368.

Wolfe, C. J., Bjarnson, I. Th., VanDecar, J. C., Solomon, S. C., Seismic structure of the Iceland mantle plume, 1997, *Nature, 385*, 245 - 247.

Table 1. Comparison of seismic (S) and gravity (G) Moho estimates from Figure 8.

Seismic Study	Symbol	W-Lon. (deg)	N-Lat. (deg)	S-Moho +/- Error (km)	G-Moho (km)
Bjarnason et al. [1993]	◆	22.1	64.5	24 +/- 2	28
	◆	21.2	64.2	21.5 +/- 2	28 [a]
	◆	20.7	64.0	21 +/- 2	26
Smallwood et al. [1999]	■	12.0	64.1	25 +/- 2	27
	■	11.0	63.5	28 +/- 2	26
	■	9.9	63.1	28 +/- 2	26
	■	8.5	62.2	35 +/- 2	30
Smallwood and White [1998]	*	27.0	61.35	10.5 +/- 2	21[a]
Staples et al. [1997]	◀	16.8	65.52	20 +/- 2	33 [a]
	◀	16.0	65.4	32 +/- 2	32
	◀	15.25	65.2	34 +/- 2	30
Kodiara et al. [1997]	+	13.85	69.7	9.2 +/- 2	21[a]
Holbrook et al. [2001]	●	32.0	67.0	33 +/- 2	30
	●	27.1	66.1	30 +/- 2	26
	●	25.0	66.0	30.3 +/- 2	29
Morgan et al. [1989]	●	18.0	58.75	27 +/- 2	30
Darbyshire et al. [1998]	▲	19.5	65.9	25 +/- 2	25
	▲	17.5	64.75	39 +/- 2	39
Weir et al. [1998]	▶	22.5	63.94	11 +/- 2	23 [a]
Holbrook [1998] [b]	▼	23.00	65.75	30 +/- 5	30

Table 1. (continued)

Seismic Study	Symbol	W-Lon. (deg)	N-Lat. (deg)	S-Moho +/- Error (km)	G-Moho (km)
Menke [1998]	★	20.17	64.05	30 +/- 2	26
	★	16.25	65.25	35 +/- 2	32 [a]
Average				26	28

[a]Seismic and gravity Moho difference may reflect partial melting.

[b]Reported by *Menke* [1998].

Figure Captions and Figures

Figure 1. North Atlantic topography and bathymetry for the region between 57.2° and 69.8°N latitude and 34°W and 2.5°W longitude. Annotations in this and subsequent maps include the amplitude range (AR), amplitude mean (AM), amplitude standard deviation (ASD), amplitude unit (AU), and grid interval (GI) and contour interval (CI). Dashed contours delineate negative values below sea level. Also shown are the locations of the neovolcanic Western (WRZ) and Eastern (ERZ) Rift Zones. This and subsequent maps were produced using the Albers equal-area conic projection.

Figure 2. Free-air gravity anomalies for the study region at 20 km elevation [*Lemoine et al.,* 1998a; b]. In this and subsequent maps, the coastlines and 1000 meter bathymetric contour are marked by heavy black lines.

Figure 3. Terrain gravity effects of the study region at 20 km elevation.

Figure 4. Terrain-correlated free-air gravity anomalies for the study region at 20 km elevation.

Figure 5. Compensated terrain gravity effects for the study region that with sign reversal yield the annihilating effects for estimating by inversion the Moho relief and related crustal thickness variations.

Figure 6. Regional modeled reduced heat flow used to scale density contrasts across the mean seismic reference depth as input for our Moho inversion estimates.

Figure 7. Comparison of synthesized mantle (lines) and observed surface heat flow marked by circles [*Flóvenz and Saemundsson,* 1993] and triangles [*Langseth et al.,* 1990]. The dash-dot line is the modeled Mid-Atlantic Ridge heat flow contribution as measured from the **ERZ**, while the dashed line is the modeled Iceland Plume heat flow contribution, and the solid line is the total modeled regional reduced heat flow. The correlation coefficient (CC) for the data is also given.

Figure 8. Gravity inferred crustal thickness variations for the study region and the seismic control points that are listed in Table 1 with the station symbols.

Figure 9. Percent mantle density reductions due to thermal expansion and partial melting in terms of excess mantle temperatures (δt).

Figure 10. Crustal cross section along 65°N latitude.

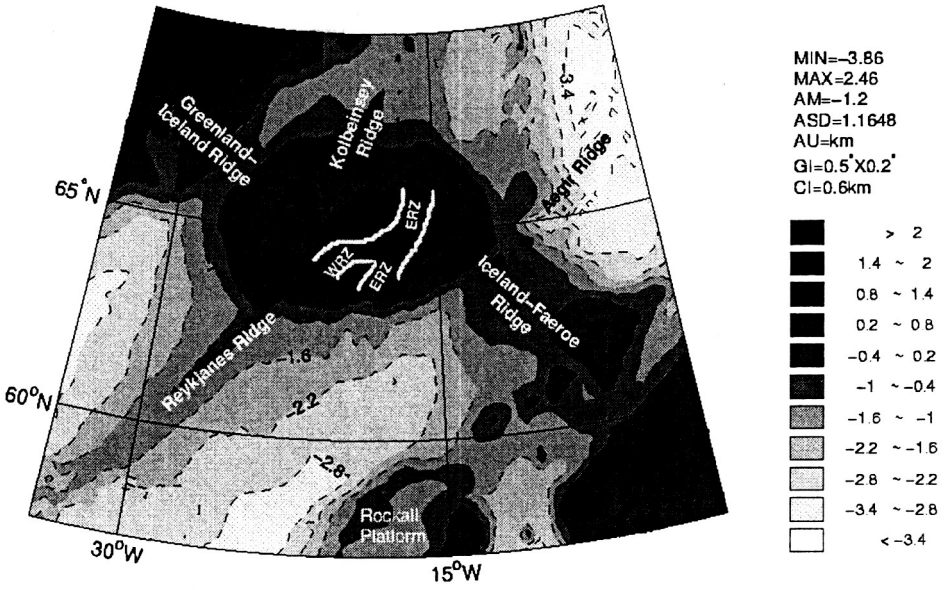

Figure 1

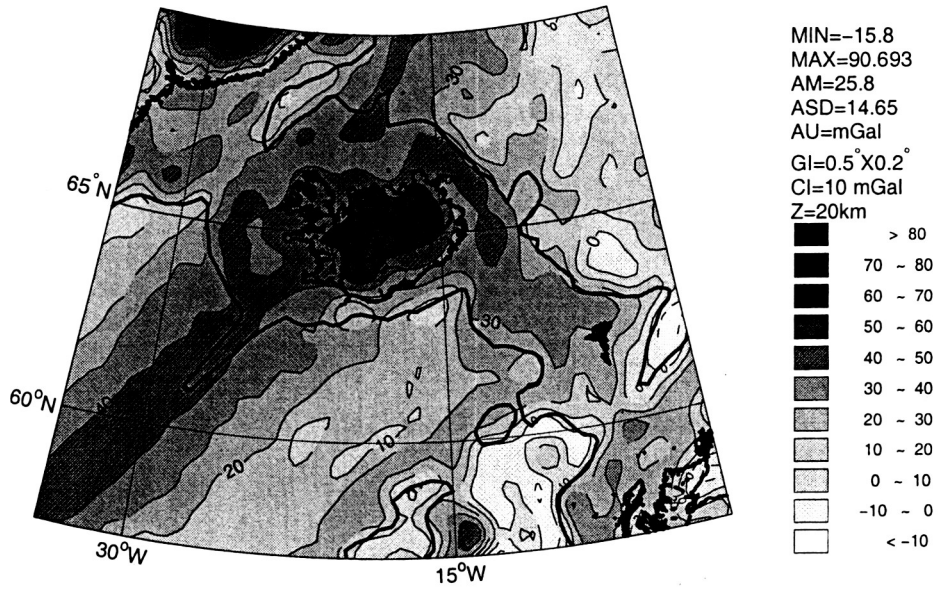

Figure 2

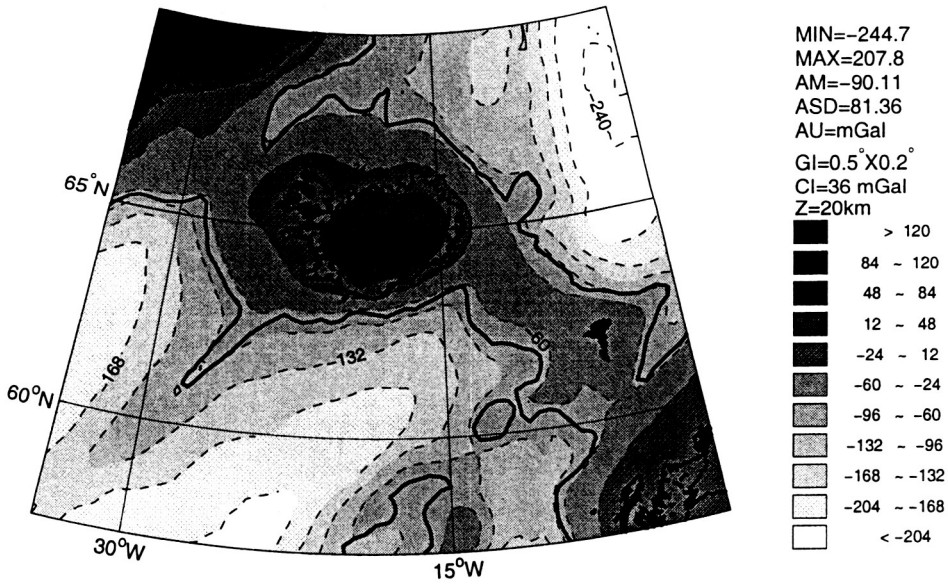

Figure 3

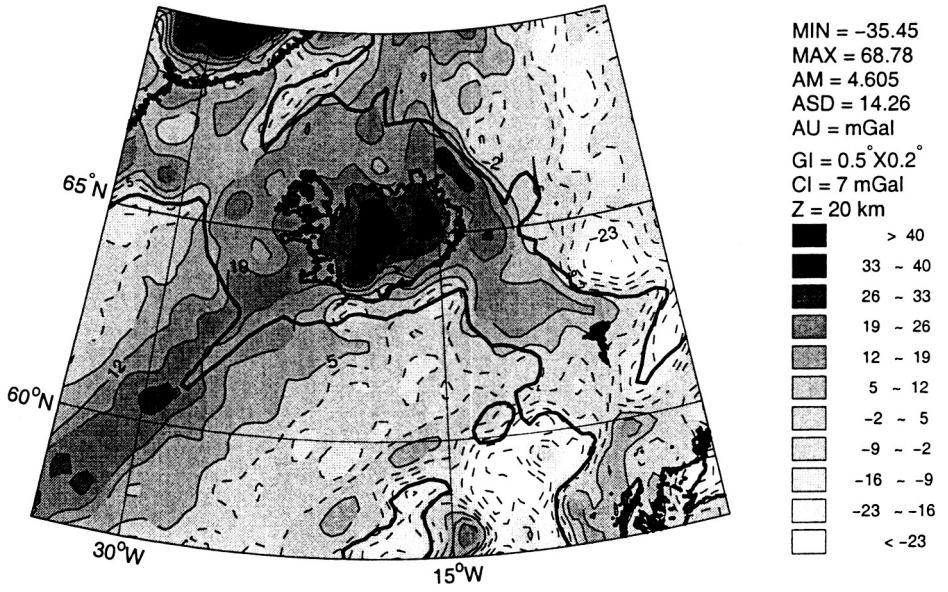

Figure 4

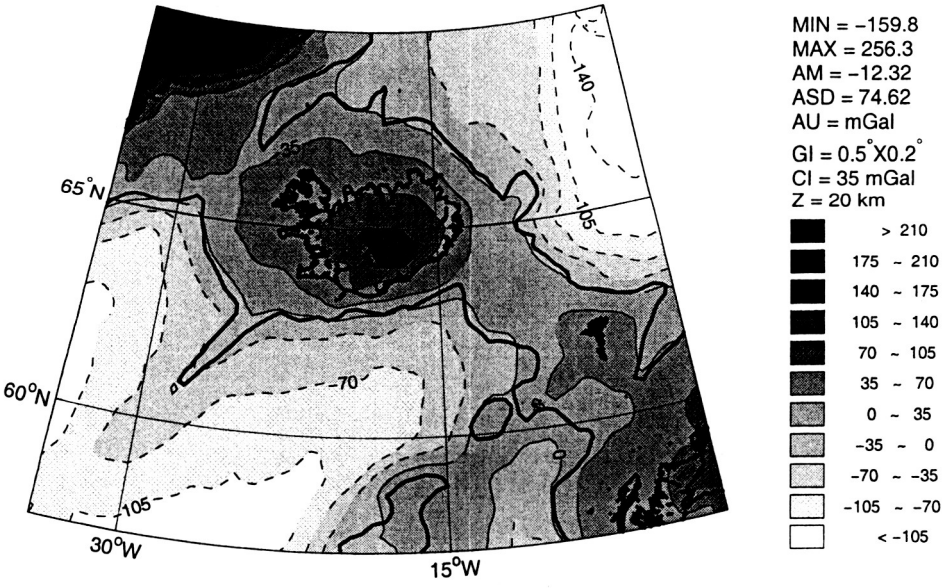

Figure 5

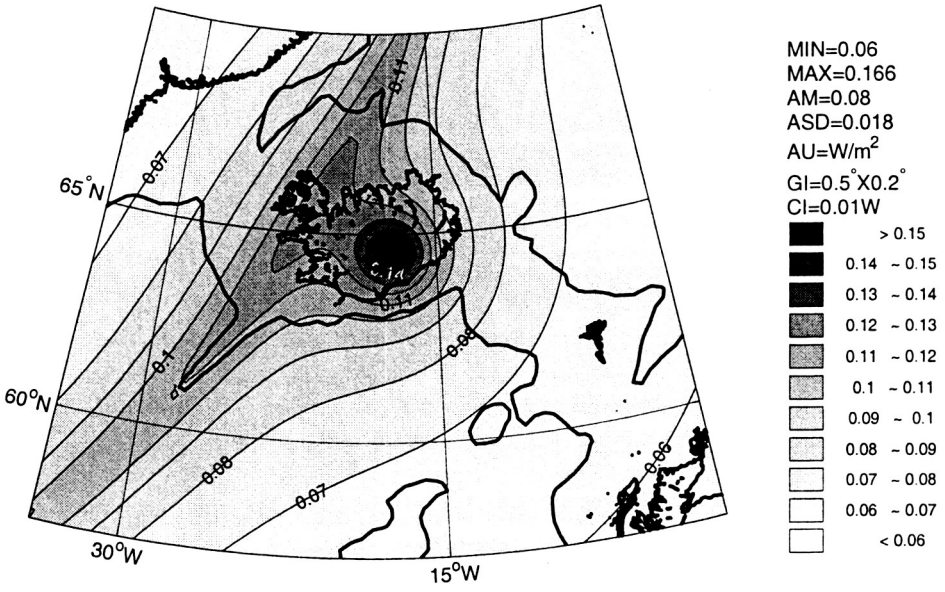

Figure 6

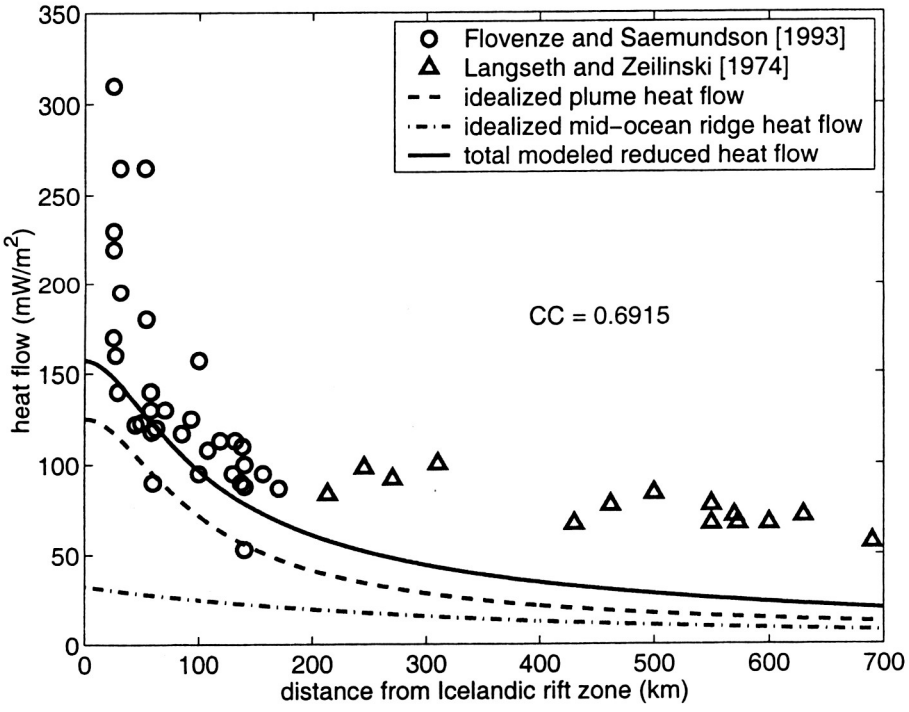

Figure 7

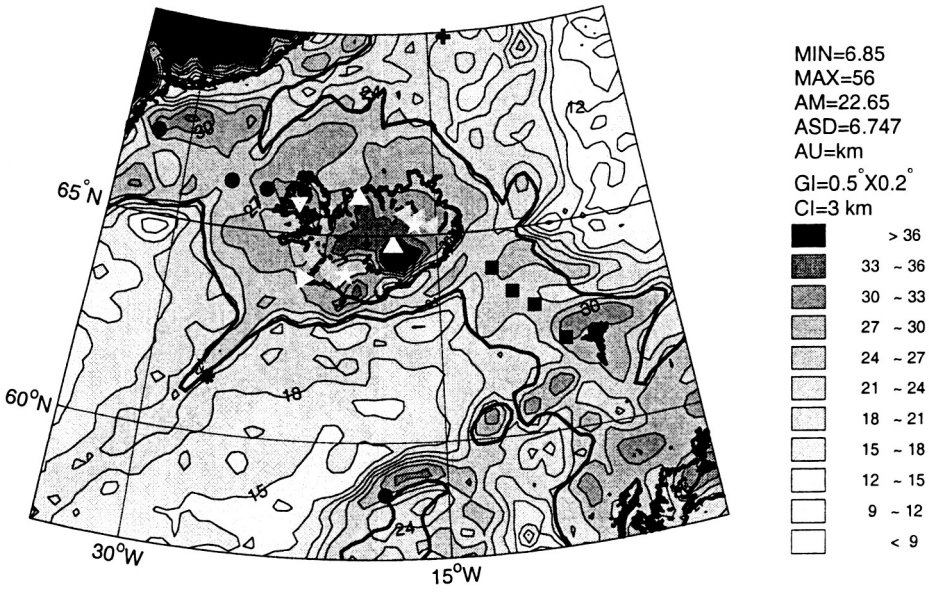

Figure 8

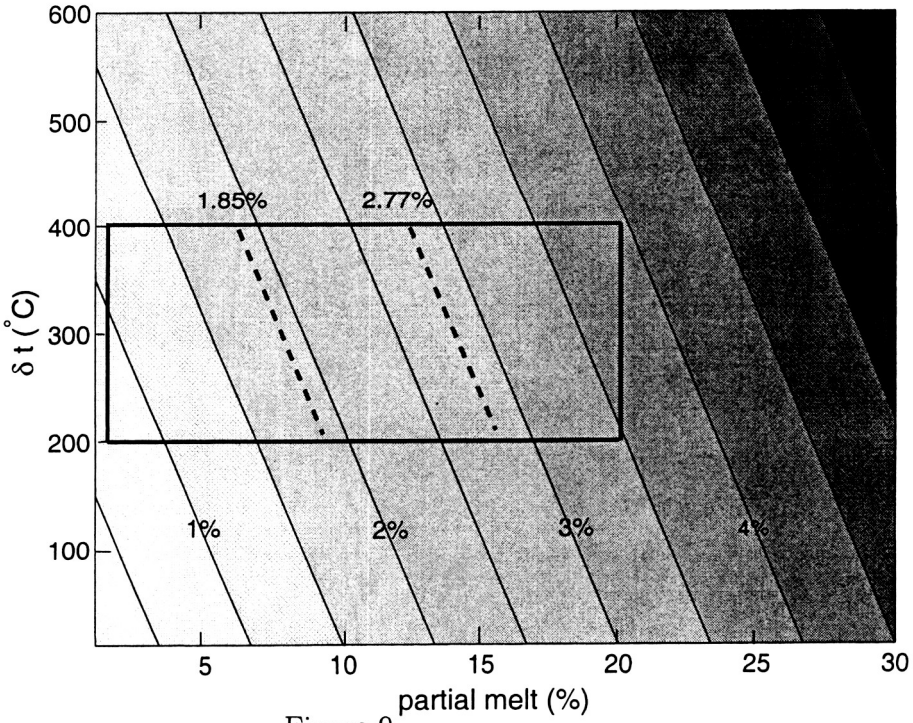

Figure 9

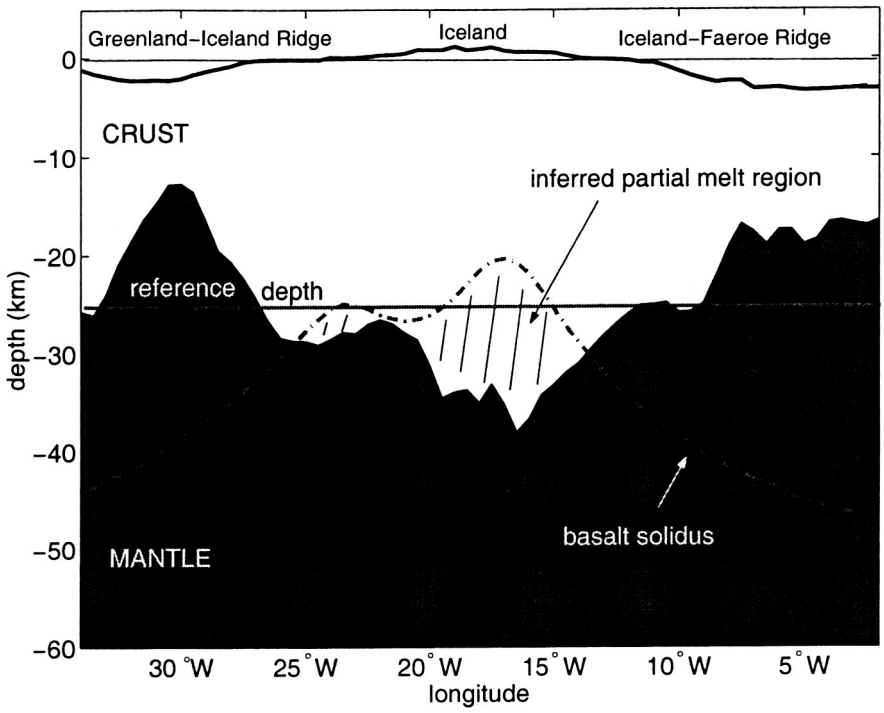
Greenland–Iceland Ridge
Iceland
Iceland–Faeroe Ridge
0
CRUST
−10
inferred partial melt region
−20
reference
depth
depth (km)
−30
−40
basalt solidus
−50
MANTLE
−60
30 °W
25 °W
20 °W
15 °W
10 °W
5 °W
longitude

Figure 10